Design of Structured Controller Satisfying H_∞ Loop Shaping using Evolutionary Optimization: Application to a Pneumatic Robot Arm

Somyot Kaitwanidvilai and Manukid Parnichkun

***Abstract*—This paper proposes a new design procedure of a fixed-structure robust controller for the joint space control of a pneumatic robot arm. The proposed technique is based on the concept of H_∞ loop shaping which is a sensible method for robust controller design. However, in conventional H_∞ loop shaping, the order of the controller is much higher than that of the plant. It is not easy to implement this controller in practical applications. To overcome this problem, in this paper, H_∞ loop shaping control under a structure-specified controller for a pneumatic robot is proposed. The performance and robust stability conditions of the designed system satisfying the H_∞ loop shaping are formulated as the objective function in the optimization problem. Genetic algorithm (GA) is adopted to solve this problem and to achieve the control parameters of the proposed controller. Additionally, in the proposed technique, the performance weighting function, which is normally difficult to obtain, is determined by using GA. The optimal stability margin is used as an objective in GA for selecting the optimal weighting parameters; the requirements in terms of performance specifications are utilized as additional constraints in order to get more practical parameters. The designed controller contains simple structure with lower order and still retains the robustness and performance specification. Simulation results show that the robustness and performance of the proposed controller are almost identical to those of the controller designed by H_∞ loop shaping method. Experimental results verify the effectiveness of the proposed technique.**

***Index Terms*—H_∞ loop shaping control, robust control, pneumatic robot, pneumatic actuator.**

I. Introduction

In the past decades, many immense developments in pneumatic controllers have been done and the results of those are used extensively in today industrial processes. Pneumatic actuator is an attractive choice for being used in both industrial and non-industrial applications because of the following advantages-high reliability, mainly because of fewer moving parts; self-cooling; high power-to-weight ratio; wide useful range; easy installation and maintenance; and, the availability of a wide range of standard sizes. Recently, this actuator has been used in the designing of the robot manipulators to enhance capabilities of the robot. Because of the advantages of this actuator, the pneumatic robot is now an attractive choice for the industrial robot.

Pneumatic system is highly nonlinear because of its compressibility of air and highly nonlinear flow through pneumatic components. Furthermore, in a long connecting tube, the effects of time delay are significant. These lead to a difficulty in analyzing and designing an effective controller for the system. Many researchers investigated various control techniques to control the system. Several approaches based on nonlinear control techniques have been successfully applied to design a controller for pneumatic system, such as block-oriented approximate feedback linearization by Fulin Xiang and Jan Wikander in 2003 [1], fuzzy state feedback control by H. Schulte and H. Hahn in 2004 [2], and etc. Unfortunately, because of time consuming in system identification process and many feedback states, these techniques are now only implemented in very precise requirement applications but not in general industrial applications. In linear control point of view, linear model is derived from linear mathematic equations. Mostly, linear dynamic model is obtained by applying the linearization technique around a specified operation point, usually at the middle of pneumatic cylinder. Various control techniques based on linear control have been proposed to control a pneumatic system such as simple PID control [3], PI control with analog loop [4], self-tuning control [5], and etc. Since these techniques do not include the presence of system uncertainties; that is, system nonlinear characteristics, load changing, and so on into the consideration in the system modeling; the robustness in the sense of uncertainties of these designed controllers cannot be guaranteed. To solve such problem, some researchers applied the robust control of a pneumatic system. Kimura and *et. al.* [6] proposed a minor feedback loop and H_∞ control to pneumatic servo. Inner pressure loop is used to reduce the complexity of resulting controller in H_∞ control. Kimura and *et. al.* [7] also applied a sampled-data H_∞ control approach into the plant. Experimental results in his work showed the advantages of discrete H_∞ control over the continuous H_∞ control in certain senses. However, in some techniques such as robust H_∞

Manuscript received October 25, 2007. This work was fully supported by Thailand Research Fund (TRF, Project No. MRG4980087), Thailand.

S. Kaitwanidvilai is with the Electrical Engineering Department, Faculty of Engineering, King Mongkut's Institute of Technology Ladkrabang, Bangkok 10520, Thailand. (Phone: 66-81-5961386, e-mail: kksomyot@kmitl.ac.th)

M. Parnichkun is with the School of Engineering and Technology, Asian Institute of Technology, Pathumtani, 12120, Thailand. (e-mail: manukid@ait.ac.th)

optimal control, the structure of controllers is complicated with a high order. It is difficult to implement these controllers in practice. Mostly, the controllers used in industrial process are PI or PID controllers. Unfortunately, tuning of control parameters of these controllers for achieving both robustness and performance specifications is difficult. To overcome this problem, the approaches to design a robust control for structure specified controller were proposed in [8-10]. In [8], a robust H_∞ optimal control problem with structure specified controller was solved by using genetic algorithm (GA). Bor-Sen.Chen. *et. al.*[9], proposed a PID design algorithm for mixed H_2/H_∞ control. In their paper, PID controller parameters were tuned in the stability domain to achieve mixed H_2/H_∞ optimal control. A similar work was also presented in [10]. In H_∞ optimal control, H_∞ loop shaping control is a feasible design method for designing a robust controller. Uncertainties in this approach are modeled as the normalized left co-prime factor which is not representing the uncertainty of the real plant. However, this approach is suited for designing a robust controller since the well known classical loop shaping concept is incorporated in the design procedure. Additionally, in the system that the dynamic model is identified by the standard system identification with black-box modeling approach, the robust control technique based on the structured uncertainty model such as mu-synthesis, H_2/H_∞ optimal control, and etc. can not be applied. However, the structure of controllers designed by H_∞ loop shaping is complicated with a high order. In this paper, genetic algorithm based fixed-structure H_∞ loop shaping control of a pneumatic robot arm is proposed. The simple structure and robust controller can be achieved. Additionally, in this paper, we propose a GA to evaluate an appropriate performance weight W_1 that satisfying the performance specifications and robustness. This then reduces the difficulty in selecting appropriate weight in H_∞ loop shaping control. The controller designed by the proposed approach has a good performance and robustness as well as simple structure. This allows our designed controller to be implemented practically and reduces the gap between the theoretical and practical approach.

The remainder of this paper is organized as follows. Pneumatic robot dynamics, pneumatic actuator dynamics are described in section II. Conventional H_∞ loop shaping and the proposed technique are discussed in section III. Section IV demonstrates the design example and results. And, finally, in section V the paper is summarized with some final remarks.

II. Dynamic Model

In this paper, we constructed a cylindrical type robot arm with pneumatic actuators. This robot is widely used in many industrial processes. Consider the cylindrical type robot arm shown in Fig.1, it is seen that it consists of two translation joints and a revolute joint. Generally, the dynamic model of this robot can be written as [11]

$$\begin{bmatrix} J+m_2r^2 & 0 & 0 \\ 0 & m_1+m_2 & 0 \\ 0 & 0 & m_2 \end{bmatrix}\begin{bmatrix} \ddot{\theta} \\ \ddot{h} \\ \ddot{r} \end{bmatrix}+\begin{bmatrix} 2m_2r\dot{r}\dot{\theta} \\ 0 \\ -m_r\dot{\theta}^2 \end{bmatrix}+\begin{bmatrix} 0 \\ (m_1+m_2)gh \\ 0 \end{bmatrix}=\begin{bmatrix} n_1 \\ f_2 \\ f_3 \end{bmatrix}$$

$$\tau=\begin{bmatrix} n_1 & f_2 & f_3 \end{bmatrix}^T \tag{1}$$

where m_1 and m_2 are the mass of the vertical and horizontal links, respectively,

θ is angle of the rotation axis,

g is gravity,

J is inertia of the base link,

h is the distance of the vertical link,

r is the distance of the horizontal link,

τ is the force vector.

n_1, f_2 and f_3 are the torque in rotation axis, force in vertical and horizontal axis, respectively.

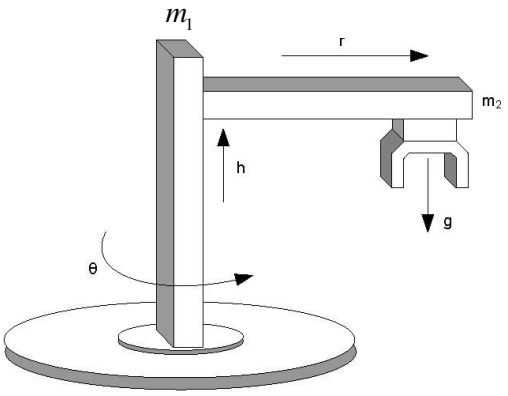

Fig.1 A cylindrical robot arm.

The dynamic model in (1) is derived from the Lagrange's equations of motion [11] and can be applied indirectly to describe the dynamic model of our developed robot.

There are many control schemes to control a robot manipulators such as computed torque control, independent joint control, and etc. In computed torque control, the control design problem is decomposed into an inner loop design and an outer loop design. The nonlinear inner loop is used to compute the inverse dynamic of the robot for canceling the nonlinear term while the outer loop control is used for trajectory tracking.

In the industrial robotic applications, *independent joint control* is widely used since it allows a decoupled analysis of the closed-loop system. At present, it is strongly accepted by several researchers that this kind of control scheme is more practically suitable for implementing in industrial robotic applications since the nonlinear control schemes used in the computed torque control scheme is too complicated to be utilized in practice. In this control scheme, each axis of the manipulators is controlled as a SISO system. Any coupling effects due to the motion of the other links are treated as disturbances. Fig. 2 shows the diagram of the independent joint control scheme. A picture of developed robot in this paper is shown in Fig. 3. Based on this control scheme, in this paper, the position of piston in each actuator of the robot is controlled separately.

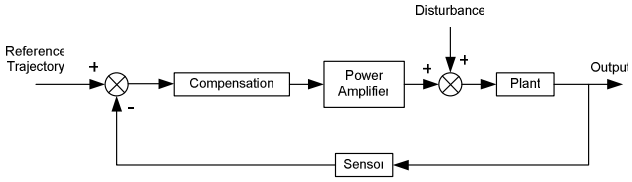

Fig. 2 Independent joint control scheme.

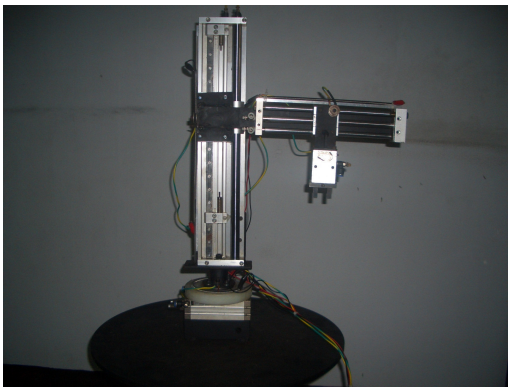

Fig.3 A pneumatically actuated robot.

In pneumatic robot, the actuator dynamics is very crucial. The foundation research works on modeling of a servo pneumatic system were derived by the study of relationship of gas properties and motion's equation in pneumatic cylinder. Linear dynamic model of a pneumatic actuator can be written as [4]

$$G(s)=\frac{y(s)}{u(s)}=\frac{k_1}{s\left(s^2+\frac{C}{M}s+k_2\right)} \tag{2}$$

where $k_1=\frac{\gamma RTG}{M}\left(\frac{A}{V_{1o}}+\frac{A}{V_{2o}}\right), k_2=\frac{\gamma}{M}\left(\frac{A^2P_{1,o}}{V_{1o}}+\frac{A^2P_{2,o}}{V_{2o}}\right)$, y(s) is position output, *u(s)* is valve's input voltage, *A* is bore area, μ is friction coefficient, *C* is viscous friction coefficient, γ is the ratio of specific heat = 1.4, V_{io} is air's volume in the chamber *i* at nominal position, *M* is total load mass, P_i is pressure in the chamber *i*, *T* is air temperature *(K)* , *R* is gas constant = 29.2 *m/K*.

To identify this model, some authors directly evaluated model's parameters by measuring the physical parameters [13, 14]. Alternatively, identification method by evaluating of the optimal model parameters to minimize the least square of prediction error can be used to identify the linear model [15].

In this paper, the standard system identification for identifying the robot dynamics is applied. Based on the concept of independent joint control scheme, the dynamic model of each axis of the robot is identified separately. The details of system identification of the developed robot are illustrated in section IV.

III. *H*∞ Loop Shaping Control and Proposed Technique

This section illustrates the concepts of the conventional H_∞ loop shaping control and the proposed technique.

A. Conventional H_∞ Loop Shaping

H_∞ loop shaping control is an efficient method to design a robust controller. This approach requires two weighting functions, W_1 (pre-compensator) and W_2 (post-compensator), for shaping the original plant G_0 so that the desired open loop shape is achieved. In this approach, the shaped plant is formulated as normalized co-prime factor, which separates the shaped plant G_s into normalized nominator N_s and denominator M_s factors [16]. Note that, $G_s=W_2G_0W_1=N_sM_s^{-1}$.

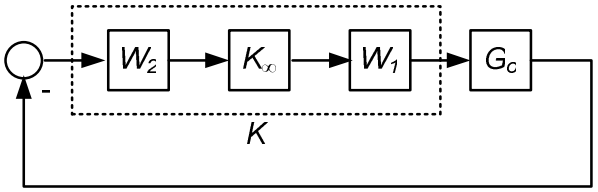

Fig.4 H_∞ loop shaping design [16].

The following steps can be applied to design the H_∞ loop shaping controller**.**

Step 1 Shape the singular values of the nominal plant G_o by using a pre-compensator W_1 and/or a post-compensator W_2 to get the desired loop shape. In SISO system, the weighting functions W_1 and W_2 can be chosen as

$$W_1=K_W\frac{s+a}{s+b} \text{ and } W_2=1 \tag{3}$$

where K_W, *a* and *b* are positive values. *b* is typically chosen as a small number (<<1) for an integral action. W_2 can be chosen as a constant since the effect of the sensor noise is negligible when the use of good sensor is assumed [17]. If the shaped plant $G_s=N_sM_s^{-1}$, the perturbed plant is written as

$$G_\Delta=(N_s+\Delta_{Ns})(M_s+\Delta_{Ms})^{-1} \tag{4}$$

Where Δ_{Ns} and Δ_{Ms} are stable, unknown representing the uncertainty satisfying $\left\|\Delta_{Ns},\Delta_{Ms}\right\|_\infty\le\varepsilon$, ε is the uncertainty boundary called stability margin. There are some guidelines for selecting the weights available in [17].

Step 2 Calculate ε_{opt} where

$$\gamma_{opt}=\varepsilon_{opt}^{-1}=\inf_{stabK}\left\|\begin{bmatrix}I\\K\end{bmatrix}(I+G_sK)^{-1}M_s^{-1}\right\|_\infty \tag{5}$$

To determine ε_{opt} , there is a unique method explained in appendix A. ε_{opt} << 1 indicates that W_1 or W_2 designed in step 1 are incompatible with robust stability requirement. To ensure the robust stability of the nominal plant, the weighting function is selected so that ε_{opt} ≥0.25 [17]. If ε_{opt} is not satisfied, then go to step 1, adjust the weighting function.

Step 3 Select ε < ε_{opt} and then synthesize a controller K_∞ that satisfies

$$\left\|\begin{bmatrix}I\\K_\infty\end{bmatrix}(I+G_sK_\infty)^{-1}M_s^{-1}\right\|_\infty\le\varepsilon^{-1} \tag{6}$$

Controller K_∞ is obtained by solving the sub-optimal control problem in (6). The details of this solving are

available in [16]. To determine M_s, there is a method explained in appendix B.

Step 4 Final controller (K) is determined as follow

$$K = W_1 K_\infty W_2 \tag{7}$$

Fig. 4 shows the controller in H_∞ loop shaping.

B. Genetic Algorithm based Fixed-Structure H_∞ Loop Shaping Optimization

In the proposed technique, GA is adopted in both weight selection and control synthesis. GA is well known as an algorithm that can be applied to any optimization problem. This algorithm applies the concept of chromosomes, and the genetic operations of crossover, mutation and reproduction. At each step, called generation, fitness value of each chromosome in population is evaluated by using fitness function. Chromosome, which has the maximum fitness value, is kept as a solution in the current generation and copied to the next generation. The new population of the next generation is obtained by performing the genetic operators such as crossover, mutation, and reproduction. In this paper, a roulette wheel method is used for chromosome selection. In this method, chromosome with high fitness value has high chance to be selected. Operation type selection, mutation, reproduction, or crossover depends on the pre-specified operation's probability. Normally, chromosome in genetic population is coded as binary number. However, for the real number problem, decoding binary number to floating number is applied [18]. The proposed technique is described in followings:

-*Weight Selection*

Weight selection is an important procedure for H_∞ loop shaping. Some researchers incorporated the performance specifications for selecting the appropriated weights [19, 20]. Based on (5), ε_{opt} can be used for indicating the compatibility of the selected weight with the robust stability requirement. However, in some cases, time domain response of close loop system at nominal plant is not satisfied although ε_{opt} is satisfied. In this paper, we specify the performance specifications and then evaluate the optimal weight W_1 by using GA. The fitness function for the weight selection is given as

$$\begin{aligned} \textit{Fitness} &= \varepsilon_{opt} \text{ if the performance specifications are satisfied,} \\ &= 0.01 \text{ (or a small value) otherwise.} \end{aligned} \tag{8}$$

A unique method to compute ε_{opt} is given in appendix A. The fitness is set to a small value (in this case is 0.01) if the performance specifications are not satisfied.

Rather than minimizing some objective functions, it is more naturally to define the performance specifications for control system design in terms of algebraic or functional inequalities. For example, in the step response, the system may be required to have a rise-time less than 0.4 s., a settling time less than 1 s. and an overshoot less than 5%. In this paper, the performance specifications are defined as

$$\begin{aligned} &\text{Maximum overshoot} < OV, \text{ Settling time} < St, \\ &\text{Steady State Error} < SE, \quad \text{Bandwidth} > BW, \\ &\text{Gain } (\omega < \omega_l) > G_u \end{aligned} \tag{9}$$

where OV, St, SE, BW, ω_l and G_u are specified values. ω is the frequency. The last term in (9) is defined for achieving good performance in some frequency range, typically some low frequency ($\omega \in [0, \omega_l]$). Other specifications can be added to achieve additional specifications.

-*Controller Synthesis*

In this paper, the genetic searching algorithm is also adopted to solve the Fixed-Structure H_∞ Loop Shaping Optimization problem. Although the proposed controller is structured, it still retains the entire robustness and performance guarantee as long as a satisfactory uncertainty boundary ε is achieved. The proposed algorithm is explained as follows.

Assume that the predefined structure controller $K(p)$ has satisfied parameters p. Based on the concept of H_∞ loop shaping, optimization goal is to find parameters p in controller $K(p)$ that minimize infinity norm from disturbances w to states z, $\|T_{zw}\|_\infty$. From (7), the controller $K(p)$ can be written as

$$K(p) = W_1 K_\infty W_2 \tag{10}$$

Assuming that W_1 and W_2 are invertible, it is obtained that

$$K_\infty = W_1^{-1} K(p) W_2^{-1} \tag{11}$$

Selecting the weight $W_2 = 1$, we get

$$K_\infty = W_1^{-1} K(p) \tag{12}$$

Substituting (12) into (6), the ∞-norm of the transfer function matrix from disturbances to states, $\|T_{zw}\|_\infty$, which is subjected to be minimized can be written as

$$J_{\cos t} = \gamma = \|T_{zw}\|_\infty = \left\| \begin{bmatrix} I \\ W_1^{-1} K(p) \end{bmatrix} (I + G_s W_1^{-1} K(p))^{-1} M_s^{-1} \right\|_\infty \tag{13}$$

The optimization problem can be written as

$$\text{Minimize } \left\| \begin{bmatrix} I \\ W_1^{-1} K(p) \end{bmatrix} (I + G_s W_1^{-1} K(p))^{-1} M_s^{-1} \right\|_\infty$$

Subject to $p_{i,min} < p_i < p_{i,max}$,

Where $p_{i,min}$ and $p_{i,max}$ are the lower and upper bounds of the parameter p_i in controller $K(p)$, respectively. Some methods for selecting the range of parameter are shown in [14-15]. The fitness function in the controller synthesis can be written as

$$\text{Fitness} = \begin{cases} \left(\left\| \begin{bmatrix} I \\ W_1^{-1} K(p) \end{bmatrix} \left(I + G_s W_1^{-1} K(p) \right)^{-1} M_s^{-1} \right\|_\infty \right)^{-1} & \text{if } K(p) \text{ stabilizes the plant} \\ 0.01 & \text{otherwise} \end{cases} \tag{14}$$

The fitness is set to a small value (in this case is 0.01) if $K(p)$ does not stabilize the plant. Our proposed algorithm is summarized as follows.

-*Weight Selection*

Step 1 Select a weight structure W_1, normally done by using (5). Define the genetic parameters such as initial population size, crossover and mutation probability, maximum generation, and etc. Also, specify the performance

specifications such as *OV, St, SE*, and etc.

Step 2 Initialize several sets of weight parameters as population in the 1st generation. If (5) is used as the weight structure, the weight parameters are K_W and a. The weight parameters are chromosome in this problem.

Step 3 Evaluate the fitness value of each chromosome using (8). Select the chromosome with maximum fitness value as a solution in the current generation. Increment the generation for a step.

Step 4 While the current generation is less than the maximum generation, create a new population using genetic operators and go to step 3. If the current generation is the maximum generation, then go to step 5.

Step 5 Check the optimal fitness value (ε_{opt}). If $\varepsilon_{opt} < 0.25$, then back to step 1 to change the weight structure and/or adjust the performance specifications if possible.

-Controller synthesis

Step 6 Select a controller structure *K(p)* and initialize several sets of parameters p as population in the 1st generation. Define the genetic parameters such as initial population size, crossover and mutation probability, maximum generation, and etc. The control parameters set, p is chromosome in GA.

Step 7 Evaluate the fitness value of each chromosome using (14). Select the chromosome with maximum fitness value as a solution in the current generation. Increment the generation for a step.

Step 8 While the current generation is less than the maximum generation, create a new population using genetic operators and go to step 7. If the current generation is the maximum generation, then stop.

Step 9 Check performances in both frequency and time domains. If the performance is not satisfied such as too low ε (too low fitness function), then go to step 6 to change the structure of controller. Low ε indicates that the selected control structure is not suitable for the problem.

IV. Simulation and Experimental Results

This section explains the design of controller for the vertical axis of a pneumatic robot. Controllers in the other axes are designed by the same design procedure. In this paper, the standard system identification using experimental data is applied to determine the dynamic model of a pneumatic robot. Based on the concept of the independent joint control scheme, the dynamic model of each axis of the robot must be identified separately. The appropriate input valve voltage signal is applied to the actuator in the axis attempted to be identified, while the pistons of actuators in other axes are maintained at the nominal positions. The estimated model is obtained when the difference between model's output, prediction, and the measured output data is minimized [15]. In this paper, an appropriate input signal was applied to the actuator in vertical axis. The data from valve's voltage input and position output are collected and used for the system identification. Simple black-box system identification was used in our work. In this approach, the structure and parameters of the plant are assumed to be unknown. Firstly, a model is selected from the standard models such as *ARMAX*, *ARX*, *OE*, and etc. Then, the orders of pole, zero, delay, and so on in the model are selected and the system identification using prediction method is applied [15]. The appropriate dynamic model can be obtained by adjusting these orders or changing the model. In this paper, to identify the plant's parameters, *"OE (output Error) model"* is selected. The details of the standard system identification and *OE model* are available in [15]. Units of output and input are meter and volt, respectively. Sampling time in our control system is 0.0112 seconds. From the procedure discussed previously, the identified plant model is found to be

$$G_0 = \frac{0.47947(s+90.76)}{(s+0.4231)(s^2+16.97s+167.9)} \tag{15}$$

Note that, this identified model includes the dynamics of actuator, valve, A/D, mass of the other links, and etc. The comparison of the simulated model output and the measured output is shown in Fig. 5. The results show that the plant model is accurately approximated by the identified model.

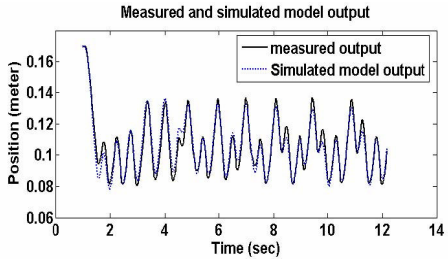

Fig.5 Comparison between simulated and measured outputs.

Based on (5), the weight parameters ranges is selected as $K_w \in [0.01, 50]$, $a \in [0.01, 50]$, $b = 0.001$. The performance specification in (9) is selected as $OV = 0.05$, $SE = 0.001$, $St = 1.2$ sec , $BW = 4$ *rad/sec* , $\omega_l = 0.4$ *rad/sec* , $G_u = 20$ *dB,* population size = 100, crossover probability = 0.7, mutation probability = 0.1, and maximum generation = 20. Fig.6 shows a plot of convergence of fitness function (optimal stability margin) versus generations by genetic algorithm. After the 12th generation, the weighting function are evaluated as

$$W_1 = \frac{15.535s+6.83}{s+0.001} \tag{16}$$

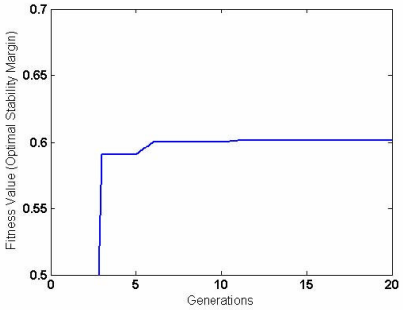

Fig.6 Convergence of the fitness value.

In the proposed technique, GA is used to evaluate the weight W_1. By using GA, the optimal stability margin (ε_{opt}) is founded to be 0.60149. This means that the evaluated weighting function is compatible with robust stability

requirement in the problem. Based on (5), $W_2 = 1$. With these weighting functions, the crossover frequency of the desired system is increased to 4 *rad/sec*. Specified time domain specifications of the system are met. Bode plots of open loop transfer function for the nominal plant and shaped plant are shown in Fig. 7. As shown in this figure, at low frequency, the open loop gain of shaped plant is much larger than that of the nominal plant. This makes the designed system good in terms of performance tracking and disturbance rejection. In this case, the shaped plant is then determined as

$$G_s = W_1 G_0 W_2 = \frac{15.535s + 6.83}{s + 0.001} \frac{0.47947(s + 90.76)}{(s + 0.4231)(s^2 + 16.67s + 167.9)} \quad (17)$$

To evaluate the performance and robustness of the proposed system, responses of the system from conventional H_∞ loop shaping (*HLS*), proposed robust PID (*PPID*), PID tuned by Ziegler-Nichols method (*ZN*) and PID tuned by Tyreus-Luyben rule (*TLC*) are investigated. We first design a controller by the conventional H_∞ loop shaping procedure. ε is set to be 0.54681, which is less than the optimal value. Then, the H_∞ loop shaping controller can be evaluated as following.

$$(HLS)K(s) = \frac{372.3s^4 + 6714s^3 + 67960s^2 + 55790s + 11950}{s^5 + 40s^4 + 701.3s^3 + 6310s^2 + 2648s + 2.641} \quad (18)$$

As shown in (18), the controller designed by H_∞ loop shaping controller is fifth order controller and complicated. It is not easy to implement practically.

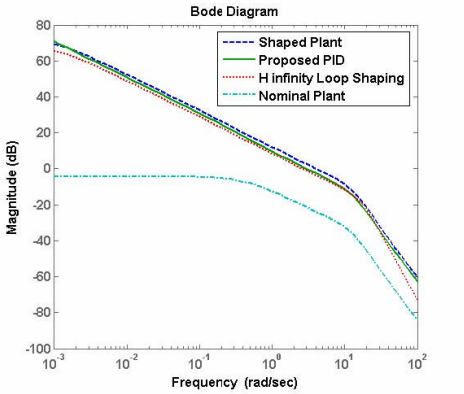

Fig.7 Bode diagram of the open loop transfer function for: the shaped plant, nominal plant, plant with *HLS*, and proposed controller.

Next, a fixed-structure robust controller using the proposed algorithms is designed. The structure of controller is selected as PID with first-order derivative filter. The controller structure is expressed in (19). K_p , K_i , K_d and τ_d are parameters to be evaluated.

$$K(p) = (K_p + \frac{K_i}{s} + \frac{K_d s}{\tau_d s + 1}) \quad (19)$$

In the optimization, the ranges of search parameters and GA parameters are set as follows: $K_p \in [0.01, 100]$, $K_i \in [0.01, 100]$, $K_d \in [0.01, 100]$, $\tau_d \in [0.01, 100]$, population size = 200 , crossover probability = 0.7 , mutation probability = 0.1 , and maximum generation = 30. As a result, the optimal controller is found to be

$$(PPID)K^*(p) = (11.013 + \frac{5.6444}{s} + \frac{38.639s}{74.162s + 1}) \quad (20)$$

Open loop bode diagram is plotted to verify the proposed algorithm. Fig. 7 shows comparison of the plant, the shaped plant, the loop shape by the proposed controller and *HLS*. As shown in this figure, both loop shapes by the proposed controller and *HLS* are close to the desired loop shape. Fig.8 shows a plot of convergence of fitness function (stability margin) versus generations by genetic algorithm. As shown in the figure, the optimal robust PID controller provides a satisfied stability margin at 0.548.

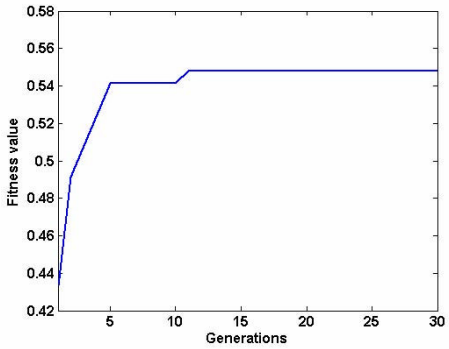

Fig.8 Convergence of the fitness value.

For performance comparison, PID tuned by *ZN* and PID tuned by *TLC* are also designed. Both tuning rules do not require an analytic model of the plant. These methods are widely used for PID tuning in many kinds of systems. In these methods, gains K_p , K_i and K_d are tuned using the ultimate gain, K_u and ultimate period, T_u. To evaluate K_u and P_u , the integral and derivative gains in PID controllers are set to zero. Ultimate gain, K_u is the proportional gain value that results in a sustained periodic oscillation in the output. Ultimate period, P_u is the period of oscillation. The details of tuning by *ZN* and *TLC* are given in [21]. Responses of the unit step input from PID controllers tuned by *ZN* and *TLC* rules are shown in Fig. 9. As seen in the figure, response from the PID tuned by *ZN* has a maximum overshoot about 45 % while there is a maximum overshoot about 10% from the PID tuned by *TLC*. Response from *TLC* is seem better than the response from *ZN*; however, both responses are not met the specified specifications.

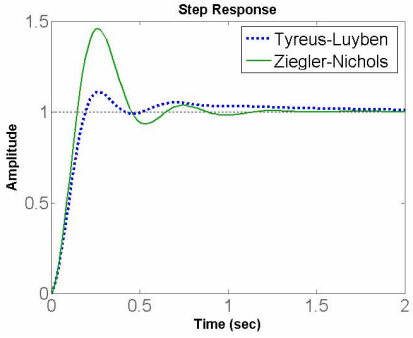

Fig. 9 Responses from the PID controller tuned by *ZN* and *TLC* tuning rules.

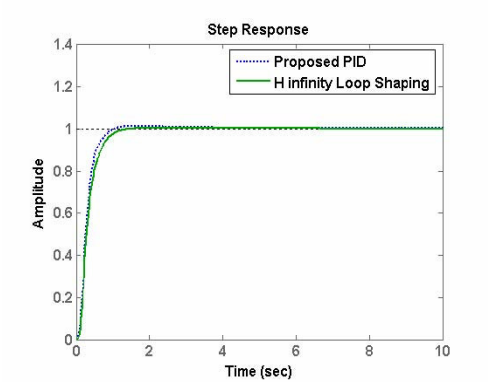

Fig.10 Step responses by the H_ loop shaping and Proposed PID.

Responses from the unit step inputs by H_∞ loop shaping (*HLS*) and the proposed robust PID (*PPID*) are shown in Fig. 10. The settling time of all responses is about 1.1 second. Response from *PPID* has a small maximum overshoot compared to the PID tuned by *ZN* and *TLC* as seen in Fig. 9. The better overshoot response is from the appropriate selection of the performance weight W_1. As shown in this figure, the settling time of *PPID* and *HLS* are almost identical. Response from the proposed controller has a small maximum overshoot about 1 % while there is no overshoot from the *HLS*.

Fig. 11 shows the closed-loop frequency domain measures relevant to this design. The common closed-loop transfer function objectives and their interpretations are shown in Table 1 [22]. The notation $\sigma(A)$ is the maximum singular value of A.

Table 1 Common closed-loop transfer function objectives [22] (Note that, in this paper, the control system is negative feedback control)

Function	Interpretation
$\bar{\sigma}\left((I+GK)^{-1}G\right)$	- Gain form input disturbance to plant output.
$\bar{\sigma}\left(GK(I+GK)^{-1}\right)$	-Gain form controller input disturbance to plant output. - $1/\bar{\sigma}\left(GK(I+GK)^{-1}\right)$ indicates the maximum allowable output multiplicative plant perturbation for closed-loop stability.
$\bar{\sigma}\left(K(I+GK)^{-1}\right)$	-Gain form output disturbance to controller output. - $1/\bar{\sigma}\left(K(I+GK)^{-1}\right)$ indicates the maximum allowable additive plant perturbation for closed-loop stability.

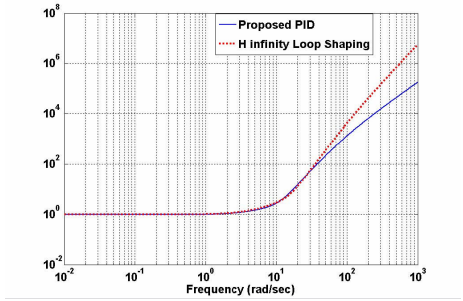

(a)

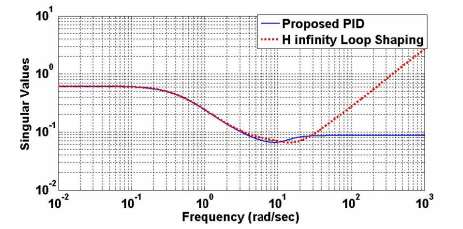

(b)

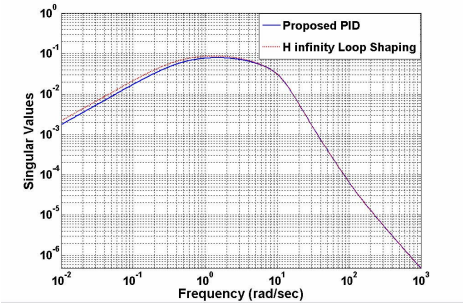

(c)

Fig.11 (a) Maximum multiplicative plant perturbation, $1/\bar{\sigma}(GK(I+KG)^{-1})$, (b) maximum allowable additive plant perturbation for close loop stability , $1/\bar{\sigma}\left(K(I+GK)^{-1}\right)$, (c) Gain from input disturbance to plant output, $\bar{\sigma}((I+KG)^{-1}G)$

As shown in Fig. 11(a), the maximum allowable multiplicative plant perturbation of the *HLS* is better than that of the proposed controller especially in the high frequency range. In the low frequency range, this maximum allowable perturbation of *HLS* and the proposed controller are almost the same. At low frequency, uncertainties of 100% of the plant magnitude can be tolerated. In Fig. 11(b) the plot of $1/\bar{\sigma}\left(K(I+GK)^{-1}\right)$ shows that the maximum allowable additive plant perturbation for close loop stability of the *HLS* is better than that of the proposed controller especially in the high frequency range. In the low frequency range, this maximum allowable perturbation of *HLS* and the proposed controller are almost the same. Fig. 11(c) shows the plots of $\bar{\sigma}((I+KG)^{-1}G)$ which is the gain from input disturbance to plant output. As shown in this figure, the disturbance rejection of the proposed technique is as good as that achieved from H_∞ loop shaping control. The maximum gain from input disturbance to plant output of the proposed technique is about 0.08. At low and high frequency, the gain is very small which means good disturbance attenuation.

Some experiments are done on a pneumatically actuated robot arm. The developed robot consists of two pneumatic cylinders (horizontal: SMC CDY1S10H-190 and Vertical: SMC-MS-B30R) and a rotary pneumatic actuator (KOGRNGI MSR 16x300). Three 5-port proportional valves used in the experiment are Festo MPYE-5-1/8-010B. Linear potentiometers and a potentiometer are used as the position sensor of the robot. Nominal supply pressure is maintained at a constant of 450 *kPa* by pressure regulator. Fig. 12 shows the photo of the proportional valve used in the experiment. The experimental result of step response of the proposed robust PID controller is shown in Fig. 13. The result is similar to the simulation result in terms of the settling time; that is, about 1 s. In simulation result as shown in Fig. 10, there is no steady state error and there is a small overshoot in the response. However, in the experimental result, the steady state error is about ±0.7 mm. and the response has no overshoot which are caused from the non-model friction dynamic, dead-zone of valve, and limitation of the sensor resolution.

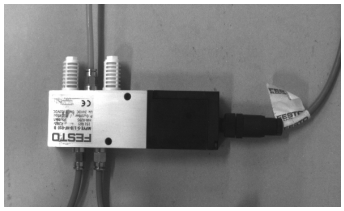

Fig.12 Photo of the proportional valve

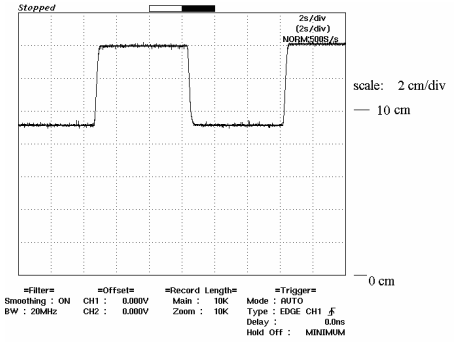

Fig.13 Response by the proposed controller in vertical axis.

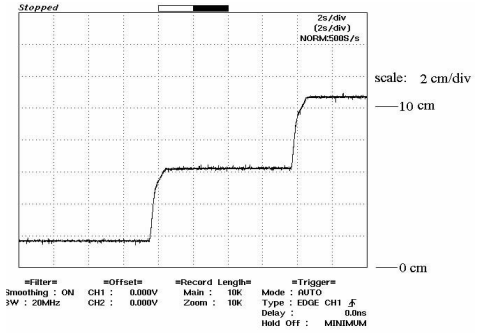

Fig.14 Response by the proposed controller in the vertical axis when the ladder input command is applied, the load at end effectors weights 3 kilograms, supply pressure is changed to 400 *kPa*, and the pistons in the actuators of other axes are moved.

Other experiment is performed to verify the robust properties of the proposed controller. The robot is used to grasp a 3-kilogram object. It is clearly shown in (1) that the changing in the load mass at the end effectors will affect the dynamic model of all axes. In this experiment, the step input commands are simultaneously applied to control the position of horizontal and rotation axes. It means that the couplings from the movement of the other links are also occurred. We also changed the supply pressure of the pneumatic system, equivalent to the parameter variation in the nominal plant. The supply pressure is changed from 450 *kPa* to 400 *kPa*. To verify the robustness of the designed system, ladder input command is applied to the position control of the vertical link. The experimental results show that the proposed controller has good robust performance from the changing of load mass and operating point. The response is almost identical to the first experiment with small difference in the setting time.

Fig. 15 shows the step responses by the proposed controller in horizontal and rotation axes. As seen in this figure, the proposed technique can be applied to design the robust controllers in any axes of a pneumatic robot.

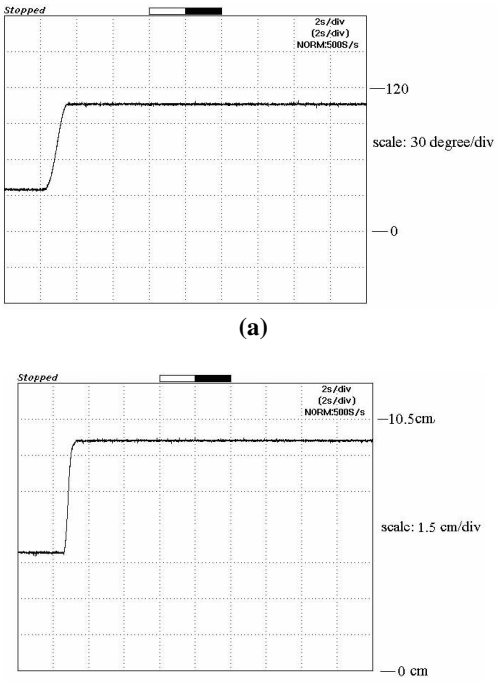

Fig.15 Step responses by the proposed controller in the (a) rotation axis (b) horizontal axis.

V. CONCLUSION

In this paper, the system identification and control of a pneumatically actuated robot was presented. When applied the standard system identification to the pneumatic system, dynamic model of each axis of a pneumatic robot can be identified. An appropriated performance weight W_1 that satisfying the time domain specifications and robustness is evaluated by GA. Based on the adequate weight selection, the responses from the proposed controller and *HLS* are better than the responses from the PID tuned by *ZN* and *TLC* rules. Although there are many approaches for PID tuning; however, our proposed technique is an alternative method which directly considers the performance specifications and

robustness in the design. Additionally, in the proposed technique, the structure of controller is not restricted to PID. The controller *K(p)* can be replaced by any fixed-structure controller and the proposed algorithm can still be applied functionally.

As shown in the simulation results, the conventional H_∞ loop shaping controller performs closer to the desired loop shape as well as the proposed controller. However, because of the complicated controller in the conventional design, the proposed approach offers a significant improvement in practical control viewpoint by simplifying the controller structure, reducing the controller order and still retaining the robust performance. Implementation in a pneumatically actuated robot assures that the proposed technique is valid and flexible. In experimental results, movements in other axes, changing of supply pressure, and the changing of load mass of the robot have a small effect to the controlled output response.

APPENDIX A

Given a shaped plant *Gs* and *A, B, C, D* represent the shaped plant in the state-space form. To determine ε_{opt}, there is a unique method as follows [17].

$$\gamma_{opt} = \varepsilon_{opt}^{-1} = (1 + \lambda_{\max}(XZ))^{1/2}$$

where *X* and *Z* are the solutions of two Riccati in (A.1) and (A.2) respectively, $\lambda_{\max}$ is the maximum eigenvalue.

$$(A - BS^{-1}D^TC)Z + Z(A - BS^{-1}D^TC)^T - ZC^TR^{-1}CZ + BS^{-1}B^T = 0 \quad \text{(A.1)}$$

$$(A - BS^{-1}D^TC)^TX + X(A - BS^{-1}D^TC) - XBS^{-1}B^TX + C^TR^{-1}C = 0 \quad \text{(A.2)}$$

Where

$$S = I + D^TD$$

$$R = I + DD^T$$

APPENDIX B

Given a shaped plant G_s and *A, B, C, D* represent the shaped plant in the state-space form. If G_s has a minimal state-space realization

$$G_s = \left[\begin{array}{c|c} A & B \\ \hline C & D \end{array}\right] \quad \text{(B.1)}$$

Then a minimal state-space realization of a normalized left coprime factorization is given by [17]

$$[N, M] = \left[\begin{array}{c|cc} A+HC & B+HD & H \\ \hline R^{-1/2}C & R^{-1/2}D & R^{-1/2} \end{array}\right] \quad \text{(B.2)}$$

Where $H = -(BD^T + ZC^T)R^{-1}$

ACKNOWLEDGMENT

The authors are sincerely thankful to Assistant. Prof. Dr. Surachet Karnprachar from Naresuan University for his useful suggestions and comments.

REFERENCES

[1] Fulin Xiang, Jan Wikander., "Block-oriented approximate feedback linearization for control of pneumatic actuator system," *Control Engineering Practice,* Vol. 12, No. 4, 2003, pp. 387-399.

[2] H. Schulte, H. Hahn., "Fuzzy State Feedback Gain Scheduling Control of Servo-Pneumatic Actuators," *Control Engineering Practice*, Vol. 12, 2004, 639-650.

[3] Ming-Chang Shih, Shy-I Tseng., "Identification and Position Control of a Servo Pneumatic Cylinder," *Control Engineering Practice*, Vol. 3, No.9, 1995, pp. 1285-1290.

[4] K. Hamiti. A. Voda-Besanqon, H. Roux-Buisson., "Position Control of a Pneumatic Actuator under the Influence of Stiction," *Control Engineering Practice*, Vol. 4., No. 8, 1996, pp. 1079-1088.

[5] Robert Richardson, Andrew R. Plummer, Michael D. Brown., "Self-Tuning Control of a Low-Friction Pneumatic Actuator Under the Influence of Gravity," *IEEE Transactions on Control Systems*, Vol. 9, No. 2, pp. 330-334.

[6] Kimura T., Hara S. and Takamori T., "H_∞ control with Mirror Feedback for a Pneumatic Actuator System," *Proceeding of 35th Conference on Decision and Control*, Kobe, Japan, 1996.

[7] Kimura T., Fujioka H. Tokai, K. and Takamori, T., "Sampled-data H_ control for a pneumatic cylinder system," *Proceeding of 35th Conference on Decision and Control*, Kobe,Japan, 1996.

[8] Bor-Sen Chen and Yu-Min Cheng., "A Structure-Specified optimal Control Design for Practical Applications: A Genetic Approach," *IEEE Trans. on Control System Technology*, Vol.6, No. 6, 1998, pp. 707-718.

[9] Bor-Sen Chen, Yu-Min Cheng and Ching-Hsiang Lee., "A Genetic Approach to Mixed H_2/H_∞ Optimal PID Control," *IEEE Trans. on Control Systems,* 1995, pp. 51-60.

[10] Shinn-Jang Ho, Shinn-Ying Ho, Ming-Hao Hung, Li-Sun Shu, and Hui-Ling Huang.Designing., "Structure-Specified Mixed H2/H Optimal Controllers Using an Intelligent Genetic Algorithm IGA," *IEEE Trans. on Control Systems*, Vol. 13, No. 6, 2005, pp. 1119-1124.

[11] F.L.Lewis, C.T. Abdallah, D.M. Dawson, *Control of robot manipulators*, New York: Macmillan, 1993.

[12] Mark W. Spong, Seth Hutchinson, M. Vidyasagar. *Robot modeling and Control*, NewYork: Jon Wiley&Sons Inc., 2006.

[13] Backe, W., Ohligschlaeger, O., "Model of heat transfer in pneumatic chambers," *Journal of Fluid Control* Vol. 20, 1989, pp. 61-78.

[14] Uebing, M, Maughan, N. D., "On Linear Modeling of a Pneumatic Servo System," *Proceeding of the Fifth Scandinavian International Conference on Fluid Power*. Vol.2, 1997, pp. 363-78.

[15] Ljung, L., *System Identification: Theory for the User,* 2nd edition, New Jersey: Prentice-Hall, 1999.

[16] Kemin Zhou, John C. Doyle., *Essential of Robust Control*, Int. ed, New Jersey: Prentice-Hall, 1998.

[17] Siguard Skogestad, Ian Postlethwaite, *Multivariable Feedback Control Analysis and Design*, 2nd ed., New York: John Wiley & Son, 1996.

[18] Mitsuo Gen, Runwei Cheng., *Genetic Algorithms and Engineering Optimization*, New York: John Wiley & Sons Inc., 2000.

[19] Da-Wei Gu, Petko H. Petkov and Mihail M. Konstantinov., *Robust Control Design with MATLAB*, London: Springer-Verlag, 2005.

[20] Alexander Lanzon., "Weight optimization in H_∞ loop-shaping," *Automatica*, Vol. 41, 2005, pp. 1201-1208.

[21] Aidan O' Dwyer, *Handbook of PI and PID Controller Tuning Rules*, 2nd ed., London: Imperial College Press, 2006.

[22] McFarlane, D.C. & K. Glover., "A loop shaping design procedure using H_ synthesis" *IEEE Trans. On Automatic Control*, Vol. 37, No. 6, 1992, pp. 759–769.